IN-89
61188

NASA Technical Memorandum 88368

Airborne Astronomy Program
Medium Altitude Missions Branch
Preprint Series 063

The Ionization Structure of the Orion Nebula: Infrared Line Observations and Models

J.P. Simpson, R.H. Rubin,
E.F. Erickson, and
M.R. Haas

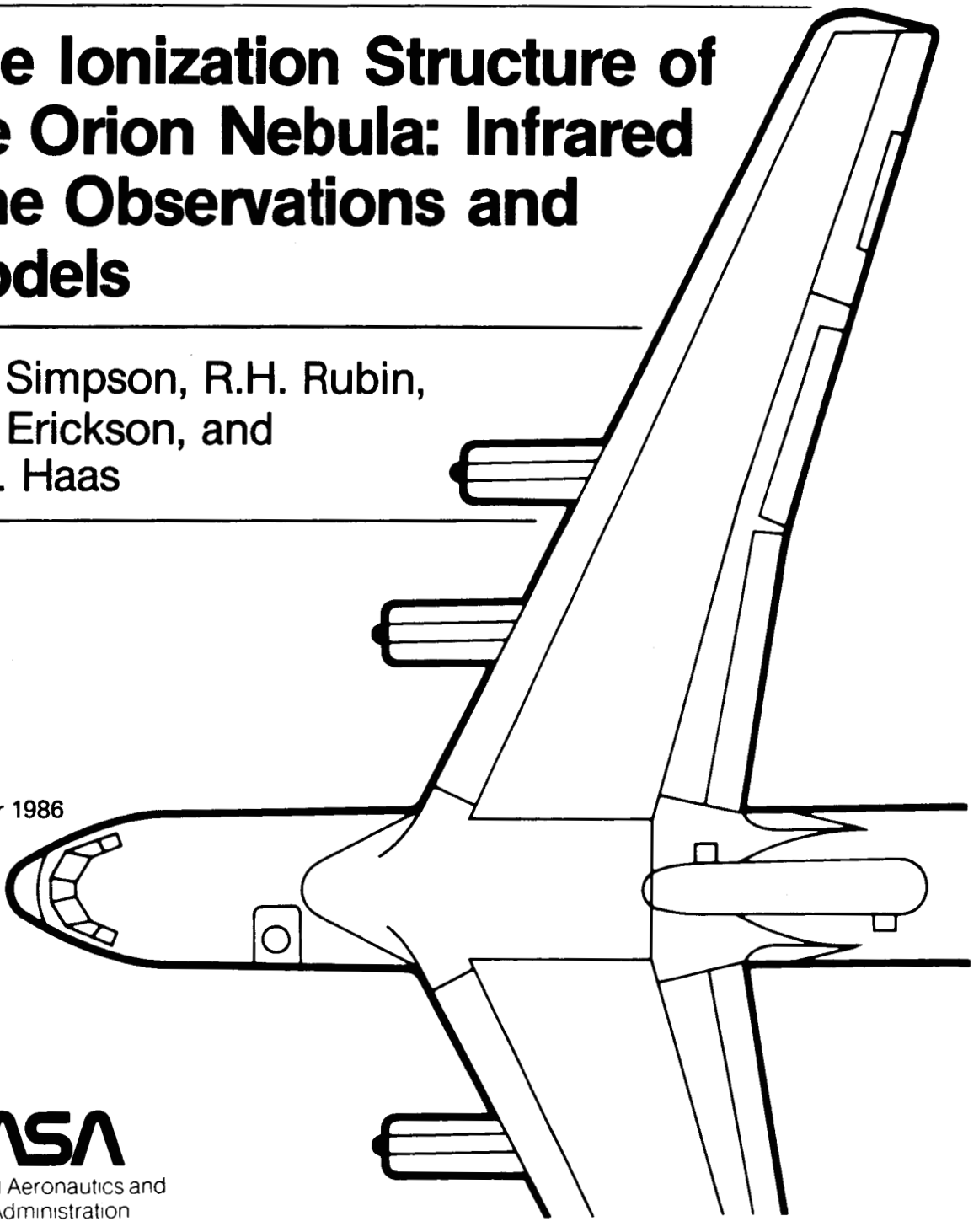

October 1986

National Aeronautics and
Space Administration

NASA Technical Memorandum 88368

Airborne Astronomy Program
Medium Altitude Missions Branch
Preprint Series 063

The Ionization Structure of the Orion Nebula: Infrared Line Observations and Models

J. P. Simpson, Lick Observatory, University of California, Santa Cruz, Califronia
R. H. Rubin, University of California, Los Angeles, California
E. F. Erickson, Ames Research Center, Moffett Field, California
M. R. Haas, Mycol, Inc., Sunnyvale, California

October 1986

National Aeronautics and
Space Administration

Ames Research Center
Moffett Field, California 94035

ABSTRACT

Observations of the [O III] 52 and 88μm lines and the [N III] 57μm line have been made at 6 positions and the [Ne III] 36μm line at 4 positions in the Orion Nebula to probe its ionization structure. The measurements, made with a ~40" diameter beam, were spaced every 45" in a line south from and including the Trapezium. The wavelength of the [Ne III] line was measured to be 36.013±0.004μm. Electron densities and abundance ratios of N^{++}/O^{++} have been calculated and compared to other radio and optical observations. Detailed one component and two component (bar plus halo) spherical models were calculated for exciting stars with effective temperatures of 37-40,000K and log g =4.0 and 4.5. Both the new infrared observations and the visible line measurements of oxygen and nitrogen require $T_{eff} \leq 37{,}000K$. However, the doubly ionized neon requires a model with $T_{eff} \geq 39{,}000K$, which is more consistent with that inferred from the radio flux or spectral type. These differences in T_{eff} are not due to effects of dust on the stellar radiation field, but are probably due to inaccuracies in the assumed stellar spectrum. The observed N^{++}/O^{++} ratio is almost twice the N^{+}/O^{+} ratio. Our best fit models give $N/H=8.4\times10^{-5}$, $O/H=4.0\times10^{-4}$, and $Ne/H=1.3\times10^{-4}$. Thus neon and nitrogen are approximately solar, but oxygen is half solar in abundance. From the infrared O^{++} lines we conclude that the ionization bar results from an increase in column depth rather than from a local density enhancement.

Subject Headings: Nebulae: H II Regions - Nebulae: Orion Nebula - Nebulae: abundances

I. INTRODUCTION

H II regions are studied in order to learn about interstellar elemental abundances and the far ultraviolet spectra of hot stars. The Orion Nebula is a case to study because it is nearby, bright, reasonably compact, the extinction is not large in the visible and is negligible in the infrared. There are radio maps available at high spatial resolution for determining the electron density. It has long been studied in the radio and visible, but only recently in the UV and infrared.

Infrared forbidden lines are important in an observational study of the structure of an H II region because some of them arise from ionization states that do not have optical forbidden lines. Such lines include transitions of N^{++} at 57μm, C^{+} at 158μm, Ne^{+} at 12.8μm, S^{+++} at 10.5μm, and Ar^{+} at 6.98μm. Additional advantages are that the lines are less affected by extinction than are the optical lines and not at all by scattering. Since infrared forbidden lines (unlike optical) are insensitive to electron temperature, the abundances determined from them depend weakly on the temperature determination. Ions with lines in both the infrared and the visible include O^{++}, Ne^{++}, S^{++}, and Ar^{++}.

One important study at optical wavelengths was done by Osterbrock and Flather (1959), who compared the intensities of Hβ, [O II] 3726 and 3729A, and [O III] 5007A out to a distance of 30 arc min from the exciting stars in the Trapezium. Spherically symmetric thermal and ionization equilibrium models such as those by Rubin (1968, 1985) and Simpson and Rubin (1984) (hereafter SR) do not reproduce these observed line ratios; that is, the ratios predicted from the models imply too few singly ionized ions in the center and too few doubly ionized ions at great distances from the exciting stars. The latter can be explained by the

fact that the Orion Nebula is also a reflection nebula, as can be seen from continuum observations. In fact, Peimbert (1982) finds that all optical lines seen farther than about 12' from the Trapezium are produced entirely by scattered light. However, due to a central hole in the dust distribution (O'Dell and Hubbard 1965, Simpson 1973, Schiffer and Mathis 1974), the inner several arc min of the nebula are negligibly affected by scattering (Peimbert 1982).

Another reason for studying the Orion Nebula is that the highly obscured, compact H II regions that have been modeled by Zeilik (1977), Herter, Helfer, and Pipher (1983), Rubin, Hollenbach and Erickson (1983) (hereafter RHE), and SR do not show the high ionization that is predicted for the hot massive stars required to match the luminosities deduced from radio observations. Possible solutions to this discrepancy are that the H II regions are excited by clusters of stars (Lacy, Beck, and Geballe 1982, RHE, SR), the ionized gas is mixed with dust that softens the stellar spectrum (Herter, Helfer, and Pipher 1983), or that the model stellar atmospheres used for the computations do not provide realistic representations of the Lyman continuum as a function of frequency and stellar effective temperature T_{eff} (RHE and Abbott and Hummer 1985). Because the Orion Nebula is nearby and relatively unobscured, we can see the exciting stars and directly determine their spectral types. It is excited predominantly by the O6p star θ^1 Ori C (Lee 1968) and several O9.5 stars that provide only a small fraction of the total flux. An O6 star supposedly has T_{eff}=40,000K (Conti 1973), although more recent work (Pottasch, Wesselius, and van Duinen 1979) prefers a lower T_{eff} (~38,000K) for this spectral type. Mathis (1985) has already suggested that T_{eff} should be lower than 40,000K for Orion, based on the O^+/O^{++} ratio. We know that there is not enough dust to affect the ionizing

spectrum in the center where there is the hole in the dust distribution. Comparison of new models of the Orion Nebula with the extensive infrared and optical observations should elucidate whether the deduced low ionization is a general problem, or whether it is confined to obscured dusty H II regions.

Another problem we wish to address is the abundance of nitrogen relative to oxygen. Because nitrogen and oxygen have similar ionization potentials, Peimbert and Costero (1969) assumed that their ionization structures are identical and that one could correct for the missing N^{++} in abundance studies of H II regions by multiplying N^+/H^+ by the ratio $(O^+ + O^{++})/ O^+$. Peimbert and Torres-Peimbert (1977) (hereafter PTP) and Torres-Peimbert, Peimbert, and Daltabuit (1980) (hereafter TPPD) studied optical lines throughout the Orion Nebula to obtain an N^+/O^+ ratio of 0.10, which they also give as the N/O ratio. However, a line from N^{++} can now be observed in the far infrared at 57μm, as can lines of O^{++} at 52 and 88μm. These three lines are mainly density sensitive (the optical lines are more sensitive to temperature), but the density can be determined from the [O III] 52/88 ratio if the lines are optically thin, which they are in all but the largest H II regions (Rubin 1968, Simpson 1975). Lester et al. (1983) in their study of these three infrared lines in several H II regions found that the N^{++}/O^{++} ratio is typically 0.2 or higher, and is 0.30 for the radio peak of the Orion Nebula itself!

N^+ does have a lower ionization potential (29eV) than O^+ (35eV), and in our H II region models (RHE; SR; Rubin 1985) the N^{++} ionization zone is larger than the O^{++} zone (except for the dense regions with T_{eff}>40,000K). Moreover, in regions excited by lower temperature stars and in regions where the matter is clumped, the ratio N^{++}/O^{++} inferred by the technique of Lester et al. (1983) is

considerably larger than the input N/O. For O6 stars like θ^1 Ori C with T_{eff}~40,000K, the N^{++} zone is similar to the O^{++} zone in a nebula of uniform density (Rubin 1985). However, the models show that the lower the effective temperature of the exciting star, the smaller the O^{++} region compared to the N^{++} region. Thus high spatial resolution observations should distinguish between an enhanced [N III]/[O III] ratio due to (a) a larger N^{++} zone than the O^{++} zone, or (b) some other factor such as different collisional excitation cross sections.

In this paper, (1) we examine the N^{++}/O^{++} ratio as a function of position in the nebula to see if it changes as the models predict. (2) We test the previous assumption that the optical line strengths are not affected by scattering in the interior several arc minutes by comparing the optical and infrared [O III] and [Ne III] intensities. (3) We investigate the problem of the overall degree of ionization being lower than predicted from the spectral type of the exciting star observed or inferred from the radio flux - a problem that was first discovered in highly obscured compact H II regions.

An investigation like this is best carried out by comparing observations and predictions of lines from several different elements with significantly different ionization potentials (such as nitrogen, oxygen, and neon). To do this in a reasonable amount of observing time, we chose not to map the entire Orion Nebula, but to observe only one sector. To be sure we had a complete sample of the ionization structure as a function of distance from the exciting star, we observed in a straight line away from the Trapezium. We chose the strip with the largest number of optical observations so that we could compare our detailed theoretical models to the singly ionized elements that have only

optical lines. We also wanted to avoid the separate H II regions around the θ^2 Ori stars (Peimbert 1982). The final choice was a line due South from the Trapezium. This included the ionization front of the bar, which we had to model as a shell of higher density, since our models are spherically symmetric. The simplification of observing and modeling only one sector has the advantage that we are not forced to average over the whole nebula; thus the chemical composition and stellar effective temperature herein derived should not be affected by the limited solid angle of the investigation.

The remainder of the paper is divided as follows: In the next section we present new observations of the far infrared transitions of O^{++}, N^{++}, and Ne^{++} in Orion. We then introduce our detailed theoretical models of the nebula in Section III. In Section IV the models are compared with our data and other published data in a detailed way. Our major conclusions are summarized in Section V.

II. OBSERVATIONS AND DATA ANALYSIS

The observations were carried out with the 91 cm telescope of the Kuiper Airborne Observatory on 1983 November 21 and 1985 February 4, 6, 12, and 14 using the facility cooled grating spectrometer (CGS) described by Erickson et al. (1984a, 1985). The aperture profiles, which were measured in the laboratory using a small blackbody source, had a FWHM of 37" in 1983 November and 46.5" in 1985 February. In both cases the beam's effective area corresponded to an equivalent disk -1.04 as large, or 2.7×10^{-8}ster in 1983 and 4.3×10^{-8}ster in 1985. The chopper throw was ~4' in azimuth (approximately E-W). Sequences of four 5 or 10s integrations were taken with the source placed alternately in

right and left beam to correct for linear variations in the background flux. In 1983 November the [O III] 51.8 and 88.4μm lines and the [N III] 57.3μm line were observed at the 6 spatial positions (P1-P6) given in Table 1. In 1985 February the same three lines were reobserved with improved signal-to-noise at positions P1, P4, P5, and P6; the [O III] 51.8μm line was observed at P7, and the [Ne III] 36.0μm line was observed at positions P1-P4. The 1985 observations are also summarized in Table 1.

The positions observed lie in a line starting at θ^1 Ori C and running straight south. Absolute positions were determined to ±5" by offsetting from either θ^1 Ori C or θ^2 Ori A. The infrared boresight was verified in flight by assuming that the 63.07μm continuum peaks at the Kleinmann-Low nebula (KL) at R.A.(1950)=$5^h32^m46.7^s$, δ(1950)=-5°24'27" (Werner 1982). The total bandpass of the six Ge:Ga photoconductor detectors was sufficient to include both the line and the adjacent continuum using a single grating position. At the different wavelengths observed the spectral resolving power was 3300-4200 in 1983 November and 2600-3300 in 1985 February.

On the 1983 November flight the absolute flux calibration and the relative detector responses were determined by observing the Mars continuum at each wavelength. The final reduced spectra are the signals obtained at the map positions divided by the signals obtained on the Mars continuum, multiplied by the flux from Mars as computed using the model of Simpson et al. (1981), and corrected for the difference in the water vapor column density. The line-of-sight water vapor was measured to be 16 precipitable microns towards Mars and 11 precipitable microns towards KL by observing a water line at 84.42μm. Since there are no strong features in the vicinity of these lines, the

resultant correction to the data was ≤5%. The [O III] line fluxes were increased by 13% because of a synchronous demodulation phase adjustment between them and the Mars calibration.

In 1985 February the absolute flux calibration and the relative detector responses were determined by observing KL on each flight in the continuum adjacent to the lines. Calibration spectra taken before and after the mapping observations on a single flight typically agreed to better than ±5%. The change in the instrument function between these nearby wavelengths was determined to ±5% using an onboard calibration source. On 1985 February 4 and 6 the line-of-sight water vapor towards KL was measured to be 9 precipitable microns by observing water lines at 60.33 and 64.22μm. This water vapor value was assumed for 1985 February 12 and 14 as well. The water vapor correction was 15±8% for [Ne III] 36.0μm, which sits on the shoulder of a relatively strong telluric water line, and ≤5% for the [O III] and [N III] lines. The final reduced spectra are the signals obtained at the map positions divided by the corresponding signals obtained on the KL continuum and multiplied by (a) the ratio of two water vapor spectra to correct for the difference in transmission, (b) the change in the instrument function, and (c) the continuum flux from KL as given by Erickson et al. (1981). At both epochs the effect of diffraction in the telescope was computed to be ≤10% and, hence, was ignored. We estimate the overall uncertainty in the absolute calibrations to be ±25%. The agreement between the two dates is consistent with this considering the different beam sizes.

The line strengths in Table 1 are the result of a nonlinear least squares fit to a flat continuum level and a superimposed Gaussian line profile

integrated over a detector bandpass. The four free parameters for the fitted curves are the line width, line height, line position, and continuum level. The line width provides a measure of the instrumental resolution since the lines are unresolved; the line position provides an estimate of the uncertainty in the wavelength calibration. For the weaker lines the width and/or position were assumed known and the line and continuum strengths were fitted. The error bars quoted in Table 1 are one-standard-deviation-of-the-mean statistical errors. The additional uncertainty in the ratio of line strengths due to systematic effects is estimated to be roughly half the absolute uncertainty quoted above for the individual line strengths.

The [Ne III] 36.0μm line was first detected by Erickson et al. (1984b) in M17 and subsequently in the planetary nebula NGC 6543 by Shure et al. (1984). The present Orion observations at positions P1-P4 are displayed in Figure 1. The line at P2 was observed using two nearby grating positions to obtain a better measurement of the continuum. From the present Orion data (V_{LSR}=-3.5km s^{-1}) and new observations of M 17 (V_{LSR}=18km s^{-1}), we find the rest wavelength of the line to be 36.013 ± 0.004μm, in agreement with our original detection.

From the [O III] 52/88μm line ratio, we have derived the electron densities N_e in Table 1 (c.f. Lester et al. 1983) using the collisional excitation cross sections of Aggarwal, Baluja, and Tully (1982). Using these densities and the 57/52μm ratio, we derived the values of N^{++}/O^{++} listed in Table 1. With the most recent cross sections for O^{++} and N^{++} (Nussbaumer and Storey 1979), the 57/52μm ratio is not very sensitive to density; the error bars for N^{++}/O^{++} are those of the 57/52μm line strength ratio. As predicted by the models discussed below, the N^{++}/O^{++} ratio does increase slightly with distance from the Trapezium

(position P1). The agreement of our data with that of other observers such as Lester et al. (1983) and Furniss et al. (1983) is adequate, considering that either our spatial positions do not agree or our beam sizes are quite different.

III. MODELS OF THE ORION NEBULA

For objects like the Orion Nebula that have a large range of electron densities and where different lines of sight sample different ionization zones, one can best study the ionization structure and chemical composition by comparison with detailed models. Our models do not include far UV or radio recombination lines, but focus on the physics of the infrared and optical lines.

a) Spherical Models

We first consider traditional spherically symmetric models. Those computed here use the H II region model program described by Rubin (1968) and updated by Rubin (1983) and SR. The electron densities of the models are those that reproduce the radio brightness maps at the same positions as our measurements (Table 1) and extending further south. The models are intended to reproduce only the observations along our cut south from the Trapezium. In Figure 2 we have plotted small beam radio brightness temperatures and the Hβ measurements of PTP scaled to 5 GHz for a line south from the Trapezium. There are two curves for Martin and Gull (1976) - the solid line is south from the Trapezium and the dashed line is south from the radio peak ($\lesssim$20" west of θ^1 Ori C). Their beam extended 20" in the north-south direction, and shows the bar clearly. A curve for the VLA map of Johnston et al. (1983) (4.8 GHz; 16"x13" beam) is also plotted. The absolute flux levels are substantially lower, no doubt because the

VLA is not sensitive to smooth extended emission. However, the general structure of the peak and bar are very similar. The map of Rodriguez and Chaisson (1978) (23.4 GHz; 80" beam) shows the sharp fall-off beyond the bar but none of the structure within the bar. The map of Wilson and Pauls (1984) (also 23 GHz; 43" beam) is similar. The other maps were made by Johnston and Hobbs (1969) (1.6' beam; 9.55mm) and by Schraml and Mezger (1969) (2' beam; 1.95cm). These last 4 maps show the outer structure of the H II region that the interferometer maps do not, but they are badly degraded by their poor resolution within about 4' from the Trapezium. The composite radio map that was used in the models reproduces the high radio peak (curve 1 for distances $\leq$0.25'), the trough and bar of curve 2 out to 2.25', and then decreases slowly from T_B~60K at 2.25' to meet the large beam fluxes at 4.5'. (The "trough" is the lower intensity region at ~1'; the "bar" is at 1.5-2.0'.) The high density maximum at the Trapezium in the model density distribution was used because our 37" and 46.5" beams include much of the radio peak, even when centered on the Trapezium star θ^1 Ori C. The small disagreement with the Hβ measurements of PTP may be due to the uncertainties in the extinction correction (approximately one magnitude) or to beam size effects. The resultant density distribution adopted for the spherically symmetric one component model is shown in Figure 3, which includes the effects of clumping as discussed below.

The physics of the models is the same as that used by SR with the addition of the new collisional excitation cross sections for [Ne II] and [Ne III] calculated by Bayes, Saraph, and Seaton (1985) and by Butler and Mendoza (1984), respectively, and new charge transfer cross sections for $O^{++}+He^{0}\rightarrow O^{+}+He^{+}$ by Butler, Heil, and Dalgarno (1984). Again we used the line-blanketed LTE model atmospheres of Kurucz (1979) for effective temperatures of 40,000K

(log g = 4.5) and 37-40,000K (log g = 4.0). The luminosities of the stars exciting the models were adjusted to give a Strömgren radius of about 8 arc min, which corresponds to the size indicated by the radio maps; the resulting Lyman continuum flux is 10^{49} photons s^{-1}. The radius of the exciting star for each model was adjusted accordingly; they range from 10.2 $R_\odot$ for T_{eff}=40,000K to 13.8 $R_\odot$ for T_{eff}=37,000K, both with log g =4.0. Models with T_{eff}=39,000K and log g =4.0 are very similar to the models with T_{eff}=40,000K and log g =4.5. Since our method determines abundances by comparing model predictions to observations, we begin with abundances taken from the literature: He/H=0.10, C/H=3.3×10^{-4}, N/H=4.5×10^{-5}, and Ar/H=4.5×10^{-6} (PTP and TPPD) and O/H=4.0×10^{-4}, Ne/H=8.1×10^{-5}, and S/H=2.2×10^{-5} (Lester, Dinerstein, and Rank 1979, hereafter LDR). We will discuss the uncertainties in these abundances later. For spherical models the gas must be clumped, since the observed line ratios that are sensitive to density imply much higher densities than implied by the computed ratios for models without clumping. We define the clumping factor as the inverse of the filling factor. A clumping factor of 4.0 was derived by considering the ratios of the [O III] 52μm and 88μm lines. It was adjusted until the average of the observed ratio equaled the average of the computed ratio for the 6 map positions. Figure 4 shows the ionization structure of the spherically symmetric model with T_{eff}=39,000K. The effect of the high density bar at 2' on the ionization is striking. Moreover, the N^{++} zone is bigger than the O^{++} zone, as expected. We note that the fraction of N^{+++} is very small.

Figure 5 compares observed optical and infrared line intensities and ratios plotted against distance from the Trapezium with model predictions. The optical line ratios were chosen because they are not as sensitive as the individual line intensities to errors in the electron density structure deduced from the

deconvolution of the radio maps. We make detailed comparison of O^+ and O^{++} lines because they characterize the ionization structure. We are also interested in the ionization structure of nitrogen. Ne^{++} is important because its 41eV ionization potential makes it extremely sensitive to the effective temperature of the exciting star. We do not discuss sulfur and argon in this paper because we do not have good observational data for all the important ionization states. The [S IV] line at 10.5μm has been a notable problem in matching theory with observations (RHE and SR) and there are no observations with a sufficiently large chopper throw. [Ar II] measurements for the Orion Nebula have not been published. Since there are no appropriate hydrogen lines to ratio to the infrared lines, the 36μm [Ne III] and the 52μm [O III] line intensities are plotted directly; like the radio continuum, they are direct functions of the luminosity of the exciting star as well as its effective temperature.

These spherically symmetric one-component models give a reasonably good account of the doubly ionized species (Figures 5a, b, c, d, and e). However, they do not describe well the singly ionized species (Figures 5f and g) at positions near the center. The observed high intensities imply many more singly ionized atoms throughout the H II region than predicted, but particularly in the central 2'. Only a model with $T_{eff} \leq 37{,}000K$ could conceivably fit the [O II] and [N II] data. In addition, the density implied by the singly ionized [O II] 3729/3726 ratio (Figure 5h) of Osterbrock and Flather (1959) and Caplan (1972) implies a density roughly 1.5 times larger than that implied by the model ratio. Since most of the O^+ is in the low density outer parts, the clumping would have to be much larger in the O^+ zone than is required for O^{++} in order to produce the observed 3729/3726 ratio. Figures 5i-o will be discussed in the next

section, where more detailed comparisons with the observations are made.

b) Bar/Halo Models

Some of the shortcomings of the one component models are probably due to their geometric simplicity; for example, Zuckerman (1973) suggested that the Orion Nebula should not be treated as spherically symmetric. As an alternative to spherically symmetric models, we derived a two component bar/halo model of the Orion Nebula which we will compare to the standard one component models discussed above. The two component model consists of two hemispheres, one in front of the star along the line of sight (also called the "halo" model) and one in back (the "bar" model) where the erosion of the molecular cloud is occurring. Each hemisphere is taken as half of a spherically symmetric model in the computation. Figure 6 is a schematic drawing of the bar/halo models. We choose this geometry as a first attempt at non-sphericity because the bar as seen in optical photographs is clearly an ionization front (see Goudis 1982 for a review) but yet there is low density ionized material extending to great distances from the Trapezium. The electron densities are given in Fig. 3. The clumping factor derived from the 52/88μm ratio for the bar/halo models is 3.0. The front hemisphere has a high density at the center, with density decreasing monotonically out to the edge. The back hemisphere starts with the same high central density, decreases sharply, but then increases again to an ionization front at 0.29pc (2' at 500pc) from the star. This reproduces the bar in projection. The bar/halo geometry reproduces the same radio flux as the one component models. The chief advantage of the bar/halo models is that the bar hemisphere has its singly ionized ions at high densities concentrated within the central 2'. The bar/halo models are also intended to reproduce only the

observations along our cut south from the Trapezium.

Figure 7 shows the predictions of the bar/halo models and the observations. (The sharp discontinuities at 2' are due to the edge of the bar.) The bar/halo models fit the data for singly ionized species significantly better than the one component models. However, it is apparent that even this departure from spherical symmetry is not sufficient to explain all aspects of the Orion Nebula; more realistic models (which are beyond the scope of this paper) are still needed. On the other hand, for doubly ionized species the two types of models give very similar answers. Although geometry can certainly explain some of the discrepancies of the predicted intensities with the observations, particularly the predicted electron density sensitive lines, we show below that other discrepancies must have other causes.

IV. DETAILED COMPARISON OF OBSERVATIONS AND MODELS

a) Oxygen

Our data, plotted in Figs. 5a and 7a, show that the bar region is less dense than the trough region, because the 52/88μm ratio decreases monotonically with distance from the Trapezium. The bar is less dense in [O II] as well (Simpson 1973). However, Figs. 5b and 7b and Table 1 show that the 52μm and 88μm intensities increase at the bar, implying a longer pathlength through the bar than through the trough, or alternatively, a smaller clumping factor in the bar. The clumping factor represents a way of accounting for inhomogeneities in models that are unrealistically simple by computational necessity. Our models assume that the clumping factor is independent of position. Moreover, because of the requirements of spherical symmetry, there is very dense bar material in the models at all lines of sight out to 2' (Fig. 6), requiring that the material

in the trough line of sight be essentially zero. The lack of agreement between the observations and the model predictions in Figs. 5a and 7a shows that spherically symmetric geometries or even our bar/halo geometry are not appropriate for the Orion Nebula. However, one can partially compensate for the inadequate geometry of the models in abundance analyses by averaging nearby points.

The predicted 3729/3726 ratio in the bar/halo models (Figs. 7h) now implies too high a density; this is undoubtably the same geometry effect discussed above (i.e. the bar is too dense).

We next compare our infrared data and the optical data of PTP, TPPD, and LDR through the ratio [O III] 52μm/5007A (Figs. 5i and 7i). This ratio was constructed from data points that overlapped spatially, albeit imperfectly. The ratio is sensitive to electron density N_e through the 52μm line and to electron temperature T_e through the 5007A line. (Higher density decreases the density sensitive line intensities through collisional de-excitation and higher electron temperature increases the intensities of the temperature sensitive forbidden lines.) The models show good agreement with the measured line ratios in the core, but the model ratios are too high in the halo. This implies that either T_e or N_e is too low in the models. The latter is not likely because the bar/halo models have higher N_e (Fig. 3) and the agreement is worse. In fact, the predicted 52/88μm ratio in the bar/halo models (Fig. 7a) shows that N_e is too high in the halo compared to our observations. The optical ratio 5007/4363A (Figs. 5j and 7j) shows that T_e is too low in all but perhaps the very centers of the models. (The 4363A line is more sensitive to electron temperature than the 5007A line because it comes from a higher energy level). The bar/halo

models are less discrepant in the cores than the one component models. Most of the discrepancy is probably due to [O III] 4363A (a favorite electron temperature indicator), because the 52/5007 and 5007/Hβ ratios, and the log of the 52μm intensities (Figs. 5i and 7i, 5d and 7d, and 5b and 7b, respectively) all agree better with the observations than does the 5007/4363 ratio. If the problem is the electron temperature in the models (rather than the cross section for the 4363A line), T_e would have to be raised from ~7000K at 2.5' from the center to over 8000K to provide the required agreement (but see the later section on neon).

The optical ratio [O II] (3726+3729)/Hβ (Figs. 5f and 7f) shows that there is not enough singly ionized oxygen, particularly in the one component model. The bar/halo model gives a better fit but not in the central 1'. The inadequacy of the model predictions cannot entirely be attributed to abundance, because plots of the [O III] 5007/Hβ (Figs. 5d and 7d) and the log of the 52μm intensity (Figs. 5b and 7b) show better agreement with the observations. Some of the excess [O II] 3727A observed in the center may be due to scattering; however, this must be a small effect because the absolute flux at 3727A is so much larger in the center than at 4' from the center. A more likely explanation is that the assumed stellar atmospheres are inappropriate. An exciting star with T_{eff}<37,000K seems to be necessary for agreement with O^+, although O^{++} agreement is better with T_{eff}=37-38,000K. If the exciting star in the models were less luminous (i.e. had a smaller radius), the O^{++} Strömgren spheres would be smaller (too small for the radio maps) and the strong decrease in [O III] intensities seen in Figs. 5b, 5d, 7b, and 7d that marks the Strömgren sphere would come at smaller distances from the Trapezium. This would help the O^{++} agreement, but not the O^+ agreement.

b) Nitrogen

As with singly ionized oxygen, the models need more singly ionized nitrogen, as can be seen in the 6584/Hβ ratio in Figs. 5g and 7g when the stellar effective temperature is >37,000K. Although scattering should not contribute as much to the intensity of the 6584A line as to that of the 3727A line (because the cross section increases as $1/\lambda$), the 6584/Hβ excess appears to be as large as the (3726+3729)/Hβ excess (Figs. 5f and 7f). The electron temperature, as determined from the 6584/5755 ratio (Figs. 5k and 7k), could be higher for the one component model, but is satisfactory for the bar/halo models, particularly in the core. Even if the electron temperatures of the models were increased within reasonable limits, thereby increasing the [N II] 6584/Hβ ratio (Figs. 5g and 7g), the models would still require more N^+. Since the input N/O ratio (0.1125) is derived from N^+/O^+, the agreement in Figs. 5ℓ and 7ℓ is expected to be good; in fact the ratio could be 15% larger in the bar/halo model, and 35% higher in the one component model. The N/O ratio for the sun is 0.1175 (Aller 1984).

On the other hand, the observed 57/52μm ratio (Figs. 5m and 7m) of N^{++}/O^{++} is about a factor of 2 larger than any model ratio in spite of the fact that the N^{++} zone is bigger than the O^{++} zone for all the models. Likewise, the derived N^{++}/O^{++} ratio is larger than the optical N^+/O^+ ratio, a problem common to other H II regions (Lester et al. 1983, Dinerstein et al. 1984). Previous proposed solutions for this discrepancy included the effects on the ionization equilibrium of having a low effective temperature for the exciting star (Rubin 1983, Dinerstein et al. 1984), a large amount of collisional de-excitation in the dense gas near the star where the ionization levels are similar (this gives

more weight to the low density material far from the star where nitrogen is more ionized than oxygen), or optical depth effects in the infrared lines (Lester et al. 1983). The models show that the differences in the N^{++} and O^{++} sampled at various lines of sight appear only at large distances (impact parameters) from the center (>2' to 3'). This eliminates the first two proposed solutions. Moreover, the agreement of the 52μm fluxes with the models (Figs. 5b and 7b) and with the 5007A line (Figs. 5i and 7i) shows that the optical depth at 52μm (and 88μm) is small. We clearly see the advantage of mapping the nebula, because we can immediately eliminate all explanations due to ionization equilibrium!

Surviving potential solutions to this problem include errors in the electron density or in the atomic data. Since [O III] 52μm and [N III] 57μm have almost the same sensitivity to electron density when the current cross sections are used, errors in the assumed electron densities are probably not the solution. If the cross sections are in error, more than one cross section must be wrong. If just the [N III] 57μm cross section were too low, raising it by a factor of two would change the intensity by only a small amount because the densities in the models are already so high that the 57μm line is collisionally de-excited to a large extent. If the cross section for the [O III] 52μm line were decreased by a factor of two, the 5007A cross section would also have to be correspondingly decreased because the 52μm/5007A ratio agrees with the observations (Fig. 7i). The agreement with the 5007/4363 ratio (Fig. 7j) would then be improved and the derived oxygen abundance would be closer to that of the sun ($O/H=8.1\times10^{-4}$, Aller 1984).

It seems most probable that the nitrogen abundance really should be a factor of two larger than that used in our models, in spite of the resulting disagreement

with the optically derived N^+/O^+ ratio (and the solar N/O ratio). If the [N II] cross sections need to be revised, those for [O II] 3726Å and 3729Å would have to be increased as well because of the apparent agreement shown in Figs. 5ℓ and 7ℓ. This would give better agreement with the [O II] 3727/Hβ ratios (Figs. 5f and 7f) as well as the [N II] 6584/Hβ ratios (Figs. 5g and 7g).

c) Neon

The [Ne III] 3869/Hβ ratio (Figs. 5e and 7e) and the plot of the log of the 36μm intensity (Figs. 5c and 7c) both require T_{eff}≈39-40,000K. One could say that the [O III] 52μm line could fit a higher temperature star too if only the inner 4 data points (to 3') were considered. However, there is little difference between the 5 models for the 52μm line in this region, and only the lower T_{eff} is consistent with the outer data points. On the other hand, there is much greater discrimination between the various models in the inner 3' region for the [Ne III] 36μm intensities than for those of [O III] 52μm. Clearly, the [Ne III] 36μm line cannot be fitted well with the 36-38,000K models that are required for oxygen and nitrogen. The optical [Ne III] and [O III] observations give the same results as the infrared, thus showing that the problem is the ionization equilibrium (or stellar atmosphere), and probably not the collisional excitation cross sections. However, the latter may be responsible for the disagreement in the electron temperatures derived from each element (the oxygen and nitrogen lines showed that the electron temperatures are too low in the models, but the [Ne III] 36μm/3869Å ratio (Figs. 5n and 7n) shows that the electron temperature is too high in the models).

Unlike nitrogen and oxygen which are mostly doubly ionized, most of the

neon in the models is in the Ne^+ ionization state. The only forbidden line of Ne^+ is at 12.8μm, where most of the ground based telescopes chop with a throw smaller than the nebula. The [Ne II] observation with the largest chopper throw (100") is that of Lester (1982;pers.comm). He measured fluxes of $8\text{-}12 \times 10^{-18}$ W cm^{-2} in 5 positions on a grid just west of θ^1 Ori C with a 10" beam. His [Ne II] fluxes are plotted in Figs. 5o and 7o. The Ne^+ intensities are well fitted by models with T_{eff}=37-38,000K. As with N^+ and O^+, there is too much singly ionized neon for the higher T_{eff} models implied by the doubly ionized species. For neon, a compromise with T_{eff}~39,000K and the Ne/H abundance higher by 20-50% fits both ionization states reasonably well. However, this T_{eff} does not agree with the oxygen and nitrogen data. A better fit might be obtained if the emergent stellar flux resembled that of the Kurucz 37,000K, log g = 4.0 model (Kurucz 1981) from 13.6eV to 41eV, but with the flux decreasing less rapidly from 41eV to 54eV.

V. SUMMARY

We present new observations of the infrared lines of [N III] 57μm and [O III] 52μm and 88μm at 6 positions and [Ne III] 36μm at 4 positions in a line south from the Trapezium in the Orion Nebula. From the data we derive electron densities and N^{++}/O^{++} ratios at all 6 positions.

We also present new models of the Orion Nebula, both spherically symmetric and two component bar/halo models, in which the electron density distributions are constrained to reproduce the high resolution radio surface brightnesses at the same positions as our data. The stellar effective temperatures range from 37,000K to 40,000K with log g=4.0 or 4.5. The stellar Lyman continuum fluxes are 10^{49} photons s^{-1}. The two-component bar/halo models give a somewhat better

account of the singly ionized atoms.

We compare the predicted intensities from the models to infrared and optical data to investigate a number of issues:

a) Elemental Abundances

The abundance ratio O/H=4.0×10^{-4} used in the models, which is approximately half solar, agrees satisfactorily with the observations. However, given the current cross sections, there is enough discrepancy between the O^{+} and the O^{++} ionization structure that the uncertainty is large. The Ne/H abundance ratio is almost certainly larger than the 8.1×10^{-5} used in the models; 1.3×10^{-4} is probably a better value, although then the Ne/O ratio would be larger than the ratio found in the sun and most planetary nebulae (Aller and Czyzak 1983, Aller 1984). Based on our [N III] and [O III] measurements we derive a N/O ratio of 0.21. The ratio from the optical [N II] and [O II] lines is N/O=0.11. [N III] and [O III] should be a better indicator of N/O because θ^{1} Ori C is hot enough that nitrogen and oxygen are mostly doubly ionized in the nebula. Because of this, we revise the nitrogen abundance upward to N/H=8.4×10^{-5}. Thus we find that nitrogen and neon are approximately solar in abundance, but compared to the sun, oxygen is underabundant. It is conceivable that the missing oxygen is tied up in dust grains, although this hypothesis has previously been rejected for the Orion Nebula (e.g. Peimbert 1982, Mathis 1985).

b) Stellar Effective Temperature

The [O III] and [N III] lines imply that the effective temperature of the exciting star is cooler than 37,000K. However, the [Ne III] lines, which are more sensitive to T_{eff}, lead us to conclude that the effective temperature is

≥39,000K for either model geometry. With no changes in abundances, the observed [Ne II], [N II], and [O II] line fluxes would require that T_{eff} be 37,000K, <37,000K, and <37,000K, respectively. However, with the higher abundances for neon and nitrogen discussed in the previous section, the singly and doubly ionized species can both be fitted by temperatures of 37,000K for nitrogen and 39,000K for neon. Oxygen cannot be fitted easily, but certainly implies $T_{eff} \leq 37,000K$. Thus in this relatively unobscured H II region, the T_{eff} derived from nitrogen and oxygen is significantly lower than the T_{eff} derived from the neon ionization. As mentioned in the introduction, in obscured H II regions the stellar effective temperature derived from the sulfur and argon ionization equilibrium is much lower than that estimated from the radio luminosity. From our additional data on neon and our mapping of the Orion Nebula in oxygen and nitrogen, we conclude that the presence of dust does not account for the inconsistencies in the methods of derivation of stellar effective temperatures. In the future, we plan to investigate other stellar spectra in the manner of RHE, such as that of a 37,000K star but with additional flux beyond 41eV to produce additional Ne^{++}. In this way, we hope to find a model that better fits the observed spectrum of the Orion Nebula.

c) Scattering by Dust

All the models show that the ratio of the singly ionized forbidden lines to Hβ increases faster than observed with distance from the center. If some of the visual flux observed in the center of the Orion Nebula is due to light scattered into the beam from positions far (>2') from the center, there would be less need for a low T_{eff} to produce the large number of singly ionized atoms observed. Scattering should be much more important for [O II] 3727A than for [N II] 6584A.

However, the two ions show similar discrepancies, leading us to conclude that scattering is not the chief cause of the large singly ionized line flux within 2' of the center, but rather, it is the ionization equilibria and abundances. However, scattering could still affect the slope of the line/Hβ ratio at the center. On the other hand, our infrared oxygen and neon data show good agreement with optical data and demonstrate that scattering is also not important for doubly ionized ions in the central 4' of the nebula.

d) Electron Densities

The measured [O III] 52/88 μm line ratios show that the enhanced intensities at the ionization bar are due to geometry effects rather than increased electron densities. We therefore do not expect our present models to reproduce the details of the density-sensitive line ratios in the vicinity of the bar. An average clumping factor for the models was derived from the far infrared [O III] lines, and the density variations in the models do reproduce the general increase in the line ratios of singly ionized ions (e.g. [O II] 3729/3726) with distance. The detailed agreement might be improved by using a different geometry/density distribution such as a blister model (Rubin 1984). We note however that the blister geometry will not account for the enhanced intensities near the bar.

e) Electron Temperature

The model electron temperatures are too high in the very center (Ne^{++} zone), but low in the O^{++} and N^{+} zones. The Ne^{++} and O^{++} zones, of course, overlap. For O^{++}, the model temperatures are worse for [O III] 5007/4363 than for [O III] 52μm/5007A. Electron temperatures are not very sensitive to T_{eff}

for the range of T_{eff} considered here. These discrepencies are possibly due to errors in the atomic parameters.

We thank the staff of the KAO for their continued support and assistance. We thank P. Duffy for his assistance with the instrument and we thank him and J. Bregman for their careful reading of the manuscript. We also thank D. Lester for giving us his data on [Ne II] in advance of publication and an anonymous referee for helpful suggestions for clarifying some points. R. H. Rubin and J. P. Simpson were supported by NASA/Ames Research Center Interchange grants NCA2-1R390-404 and NCA2-1R690-404 respectively.

TABLE 1

INFRARED LINE OBSERVATIONS OF THE ORION NEBULA

Position $\alpha(1950)$ $\delta(1950)$	Species	Line (μm)	November 1983; 37" FWHM			February 1985; 47" FWHM		
			Flux (10^{-17}W/cm^2)	Ratio 52/88 N_e (cm^{-3})	N^{++}/O^{++}	Flux (10^{-17}W/cm^2)	Ratio 52/88 N_e(cm^{-3})	N^{++}/O^{++}
P1	[O III]	52	20.8 ± 0.3	6.1 ± 0.2	0.23 ± 0.02	38.2 ± 0.3	6.0 ± 0.2	0.20 ± 0.01
5 32 49	[O III]	88	3.4 ± 0.1	4570 ± 320		6.3 ± 0.2	4370 ± 300	
-5 25 16	[N III]	57	2.8 ± 0.2			4.5 ± 0.2		
	[Ne III]	36				6.1 ± 0.2		
P2	[O III]	52	15.4 ± 0.5	5.0 ± 0.2	0.23 ± 0.03			
5 32 49	[O III]	88	3.1 ± 0.1	2950 ± 250				
-5 26 01	[N III]	57	2.2 ± 0.3					
	[Ne III]	36				3.1 ± 0.3		
P3	[O III]	52	14.8 ± 0.3	3.9 ± 0.2	0.22 ± 0.02			
5 32 49	[O III]	88	3.8 ± 0.1	1820 ± 150				
-5 26 46	[N III]	57	2.1 ± 0.2	|				
	[Ne III]	36				2.2 ± 0.2		
P4	[O III]	52	5.5 ± 0.3	3.2 ± 0.2	0.28 ± 0.05	11.5 ± 0.2	3.1 ± 0.1	0.29 ± 0.01
5 32 49	[O III]	88	1.7 ± 0.1	1320 ± 140		3.7 ± 0.1	1260 ± 70	
-5 27 31	[N III]	57	1.0 ± 0.2			2.3 ± 0.1		
	[Ne III]	36				0.7 ± 0.2		
P5	[O III]	52	1.1 ± 0.3	1.7 ± 0.4	0.54 ± 0.19	2.2 ± 0.1	2.0 ± 0.1	0.36 ± 0.03
5 32 49	[O III]	88	0.6 ± 0.1	460 ± 190		1.11 ± 0.04	600 ± 50	
-5 28 16	[N III]	57	0.5 ± 0.1			0.62 ± 0.04		
P6	[O III]	52	0.6 ± 0.3			0.55 ± 0.07	2.3 ± 0.3	0.20 ± 0.08
5 32 49	[O III]	88	<0.2 ± (3σ)			0.24 ± 0.02	760 ± 170	
-5 29 01	[N III]	57				0.08 ± 0.03		
P7	[O III]	52				<0.1 (3σ)		
5 32 49								
-5 29 46								

REFERENCES

Abbott, D.C., and Hummer,D.G. 1985, Ap.J., 294, 286.

Aggarwal, K.M., Baluja, K.L., and Tully, J.A., 1982, M.N.R.A.S., 201, 923.

Aller, L.H. 1984, Physics of Thermal Gaseous Nebulae (Physical Processes in Gaseous Nebulae), Astrophysics and Space Science Library 112 (Dordrecht: Reidel).

Aller, L.H., and Czyzak, S.J. 1983, Ap.J. Suppl., 51, 211.

Bayes, F.A., Saraph, H.E., and Seaton, M.J. 1985, M.N.R.A.S., 215, 85P.

Butler, S.E., Heil, T.G., and Dalgarno, A. 1984, J.Chem.Phys., 80, 4986.

Butler, K., and Mendoza, C. 1984, M.N.R.A.S., 208, 17P.

Caplan, J.G. 1972, Astr.Ap., 18, 404.

Conti, P.S. 1973, Ap.J., 179, 181.

Dinerstein, H., Lester, D., Werner, M., Watson, D., Genzel, R., and Rubin, R. 1984, NASA/A.S.P. Airborne Astronomy Symposium, NASA CP-2353, eds. H.A. Thronson and E.F. Erickson, p. 266.

Erickson, E.F., Knacke, R.F., Tokunaga, A.T., and Haas, M.R. 1981, Ap.J., 245, 148.

Erickson, E. F., Houck, J. R., Harwit, M. O., Rank, D. M., Haas, M. R., Hollenbach, D. J., Simpson, J. P., Augason, G. C., and McKibbin, D. D. 1984a, Airborne Astronomy Symposium, NASA CP-2353, eds. H.A. Thronson and E.F. Erickson, p. 313.

Erickson, E.F., Haas, M.R., Simpson, J.P., Duffy,P., Rubin, R.H., and Houck, J.R. 1984b, Bull.A.A.S., 15, 928.

Erickson, E. F., Matthews, S., Augason, G. C., Houck, J. R., Rank, D. M., and Haas, M. R. 1985, Proceedings of the Society of Photo-Optical Instrumentation Engineers, 509, 129.

Furniss, I., Jennings, R.E., King, K.J., Lightfoot, J.F., Emery, R.J., Naylor, D.A., and Fitton, B. 1983, M.N.R.A.S., 202, 859.

Goudis, C. 1982, The Orion Complex: A Case Study of Interstellar Matter, Astrophysics and Space Science Library 90 (Dordrecht: Reidel).

Herter, T., Helfer, H.L., and Pipher, J.L. 1983, Astr.Ap.Suppl., 51, 195.

Johnston, K.J., and Hobbs, R.W. 1969, Ap.J., 158, 145.

Johnston, K.J., Palmer, P., Wilson, T.L., and Bieging, J.H. 1983, Ap.J., 271, L89.

Kurucz, R.L. 1979, Ap.J. Suppl., 40, 1.

Lacy, J.H., Beck, S.C., and Geballe, T.R. 1982, Ap.J., 255, 510.

Lee, T.A. 1968, Ap.J., 152, 913.

Lester, D.F., Dinerstein, H.L., and Rank, D.M. 1979, Ap.J., 232, 139 (LDR).

Lester, D.F., Dinerstein, H.L., Werner, M.W., Watson, D.M., and Genzel, R.L. 1983, Ap.J., 271, 618.

Martin, A.H.M., and Gull, S.F. 1976, M.N.R.A.S., 175, 235.

Mathis, J.S. 1985, Ap.J., 291, 247.

Nussbaumer, H., and Storey, P.J. 1979, Astr.Ap., 71, L5.

O'Dell, C.R., and Hubbard, W.B. 1965, Ap.J., 142, 591.

Osterbrock, D., and Flather, E. 1959, Ap.J., 129, 26.

Peimbert, M. 1982, Symposium on the Orion Nebula to Honor Henry Draper, Annals of the New York Academy of Science, 395, eds. A.E. Glassgold, P.J. Huggins, and E.L. Schucking, New York, p. 24.

Peimbert, M., and Costero, R. 1969, Bol.Obs.Ton.Tac., 5, 3.

Peimbert, M., and Torres-Peimbert, S. 1977, M.N.R.A.S., 179, 217 (PTP).

Pottasch, S.R., Wesselius, P.R., and van Duinen, R.J. 1979, Astr.Ap., 77, 189.

Rodriguez, L.F., and Chaisson, E.J. 1978, Ap.J., 221, 816.

Rubin, R.H. 1968, Ap.J., 153, 761.

_____ 1983, Ap.J., 274, 671.

_____ 1984, Ap.J., 287, 653.

_____ 1985, Ap.J. Suppl., 57, 349.

Rubin, R.H., Hollenbach, D.J., and Erickson, E.F. 1983, Ap.J., 265, 39 (RHE).

Schiffer, F.H.,III, and Mathis, J.S. 1974, Ap.J., 194, 597.

Schraml, J., and Mezger, P.G. 1969, Ap.J., 156, 269.

Shure, M.A., Houck, J.R., Gull, G.E., and Herter, T. 1984, Ap.J., 281, L29.

Simpson, J.P. 1973, Publ.A.S.P., 85, 479.

_____ 1975, Astr.Ap., 39, 43.

Simpson, J.P., Cuzzi, J.N., Erickson, E.F., Strecker, D.W., and Tokunaga, A.T. 1981, Icarus, 48, 230.

Simpson, J.P., Haas, M.R., Rubin, R.H., and Erickson, E.F. 1984, Airborne Astronomy Symposium, NASA CP-2353, eds. H.A. Thronson and E.F. Erickson, p. 148.

Simpson, J.P., and Rubin, R.H. 1984, Ap.J., 281, 184 (SR).

Torres-Peimbert, S., Peimbert, M., and Daltabuit, E. 1980, Ap.J., 238, 133 (TPPD).

Werner, M. W. 1982, Symposium on the Orion Nebula to Honor Henry Draper, Annals of the New York Academy of Sciences, 395, eds. A.E. Glassgold, P.J. Huggins, and E.L. Schucking, New York, p. 79.

Wilson, T.L., and Pauls, T. 1984, Astr.Ap., 138, 225.

Zeilik, M., II 1977, Ap.J., 213, 58.

Zuckerman, B. 1973, Ap.J., 183, 863.

FIGURE CAPTIONS

Fig. 1. The [Ne III] lines at 36μm at each of the four positions P1-P4 (top to bottom).

Fig. 2. The radio brightness temperature scaled to 5 GHz for a cut south from the Trapezium. The Hβ measurements of PTP as scaled to 5 GHz are also plotted.

Fig. 3. The electron densities in the clumps as a function of distance from the exciting star. The units of the abcissa are 0.145pc, which corresponds to 1' at a distance of 500pc.

Fig. 4. The ionization structure in nitrogen, oxygen and neon as a function of distance from the center for the one component model with T_{eff}=39,000K. The units of the abcissa are 0.145pc, which corresponds to 1' at a distance of 500pc.

Fig. 5. Line intensities, or intensity ratios, for the five different models as functions of distance from the center of the model. The observed data are also plotted as functions of distance from the Trapezium. With exceptions as noted, the squares are our data of November, 1983, and the triangles are our data of February, 1985. Where no error bars are plotted for our data, the error bars are smaller than the size of the plotted squares or triangles. The circles are the visible data of PTP and TPPD, and the diamonds are the visible data of LDR. Fig. 5a. The ratio of [O III] 52/88μm.

Fig. 5b. The log of the [O III] 52μm intensities.

Fig. 5c. The log of the [Ne III] 36μm intensities.

Fig. 5d. The ratio of [O III] 5007A/Hβ.

Fig. 5e. The ratio of [Ne III] 3869Å/Hβ.

Fig. 5f. The ratio of [O II] (3726+3729)Å/Hβ.

Fig. 5g. The ratio of [N II] 6584Å/Hβ. The triangle is from O'Dell and Hubbard (1965).

Fig. 5h. The ratio of [O II] 3729/3726Å. The circles are from Osterbrock and Flather (1959), the squares are from Simpson (1973), and the x's are from Caplan (1972).

Fig. 5i. The ratio of [O III] 52μm/5007Å.

Fig. 5j. The ratio of [O III] 5007/4363Å.

Fig. 5k. The ratio of [N II] 6584/5755Å.

Fig. 5ℓ. The ratio of [N II] 6584Å/[O II] (3726+3729)Å.

Fig. 5m. The ratio of [N III] 57μm/[O III] 52μm.

Fig. 5n. The ratio of [Ne III] 36μm/3869Å.

Fig. 5o. The log of the intensity of [Ne II] 12.8μm.

Fig. 6. Schematic drawing of the bar/halo models.

Fig. 7. The same as Fig. 5 for the bar/halo models. Fig. 7a. The ratio of [O III] 52/88μm.

Fig. 7b. The log of the [O III] 52μm intensities.

Fig. 7c. The log of the [Ne III] 36μm intensities.

Fig. 7d. The ratio of [O III] 5007Å/Hβ.

Fig. 7e. The ratio of [Ne III] 3869Å/Hβ.

Fig. 7f. The ratio of [O II] (3726+3729)Å/Hβ.

Fig. 7g. The ratio of [N II] 6584Å/Hβ.

Fig. 7h. The ratio of [O II] 3729/3726Å.

Fig. 7i. The ratio of [O III] 52μm/5007Å.

Fig. 7j. The ratio of [O III] 5007/4363Å.

Fig. 7k. The ratio of [N II] 6584/5755A.

Fig. 7ℓ. The ratio of [N II] 6584A/[O II] (3726+3729)A.

Fig. 7m. The ratio of [N III] 57μm/[O III] 52μm.

Fig. 7n. The ratio of [Ne III] 36μm/3869A.

Fig. 7o. The log of the intensity of [Ne II] 12.8μm.

ADDRESSES OF AUTHORS

Edwin F. Erickson, Michael R. Haas, Robert H. Rubin, and Janet P. Simpson:
Astrophysical Experiments Branch, MS-245-6, NASA/Ames Research Center,
Moffett Field, CA 94025

Fig. 1

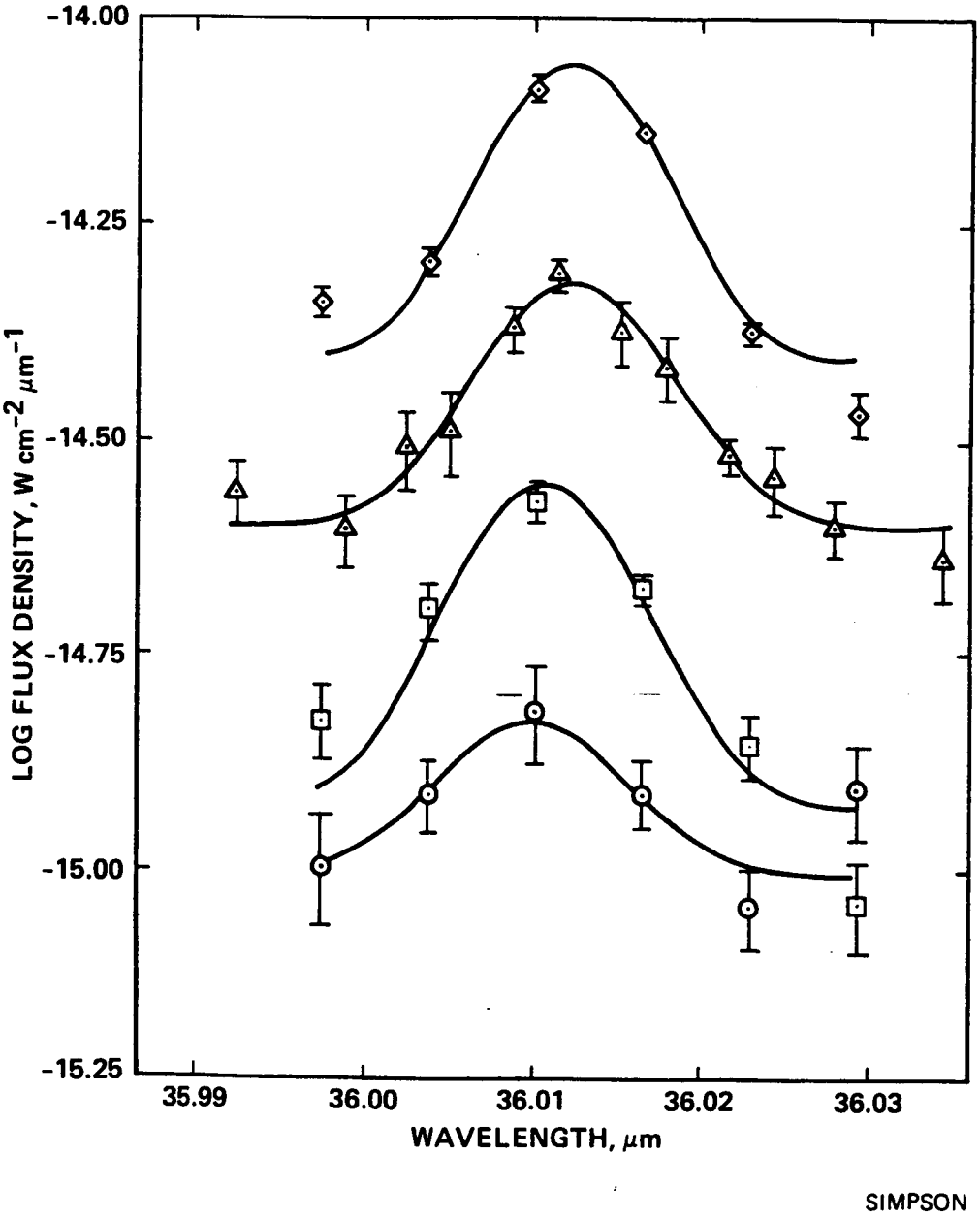
-14.00
-14.25
-14.50
-14.75
-15.00
-15.25
LOG FLUX DENSITY, W cm^{-2} μm^{-1}
35.99
36.00
36.01
36.02
36.03
WAVELENGTH, μm
SIMPSON

Fig. 2

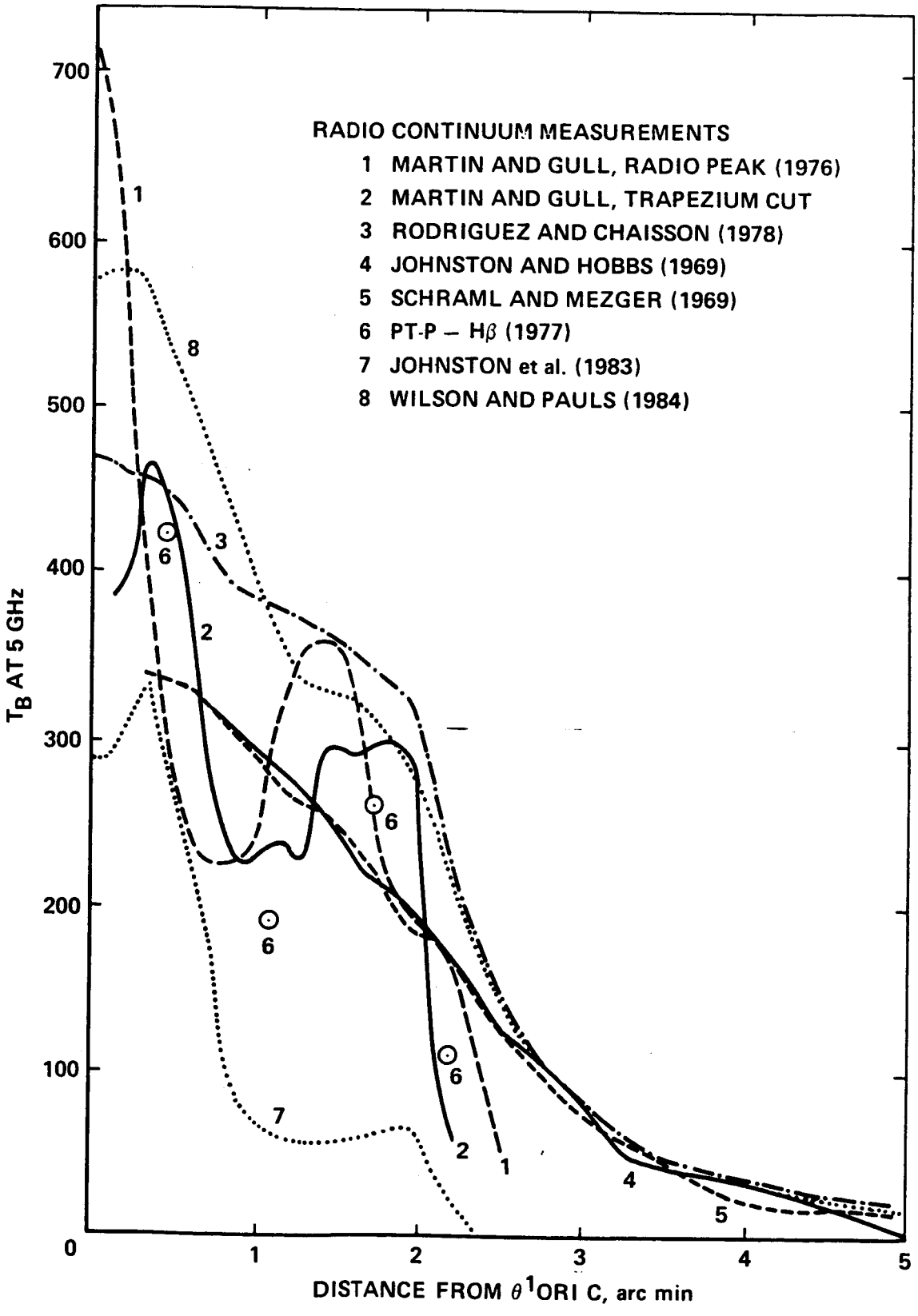
RADIO CONTINUUM MEASUREMENTS
1 MARTIN AND GULL, RADIO PEAK (1976)
2 MARTIN AND GULL, TRAPEZIUM CUT
3 RODRIGUEZ AND CHAISSON (1978)
4 JOHNSTON AND HOBBS (1969)
5 SCHRAML AND MEZGER (1969)
6 PT-P – Hβ (1977)
7 JOHNSTON et al. (1983)
8 WILSON AND PAULS (1984)
T_B AT 5 GHz
DISTANCE FROM θ¹ORI C, arc min
0
100
200
300
400
500
600
700
1
2
3
4
5

Fig 3

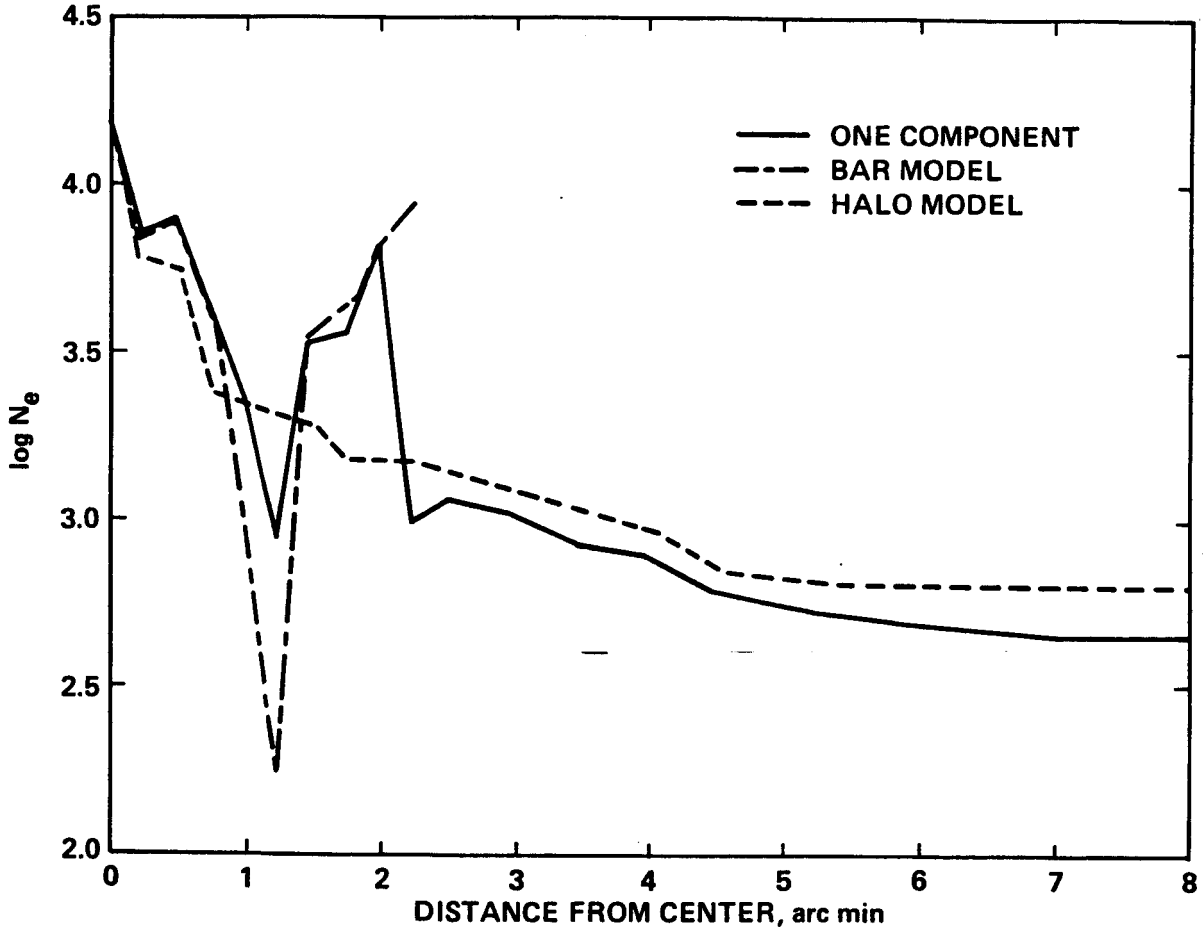
4.5
4.0
3.5
3.0
2.5
2.0
log N_e
0
1
2
3
4
5
6
7
8
DISTANCE FROM CENTER, arc min
ONE COMPONENT
BAR MODEL
HALO MODEL
SIMPSON

Fig 4

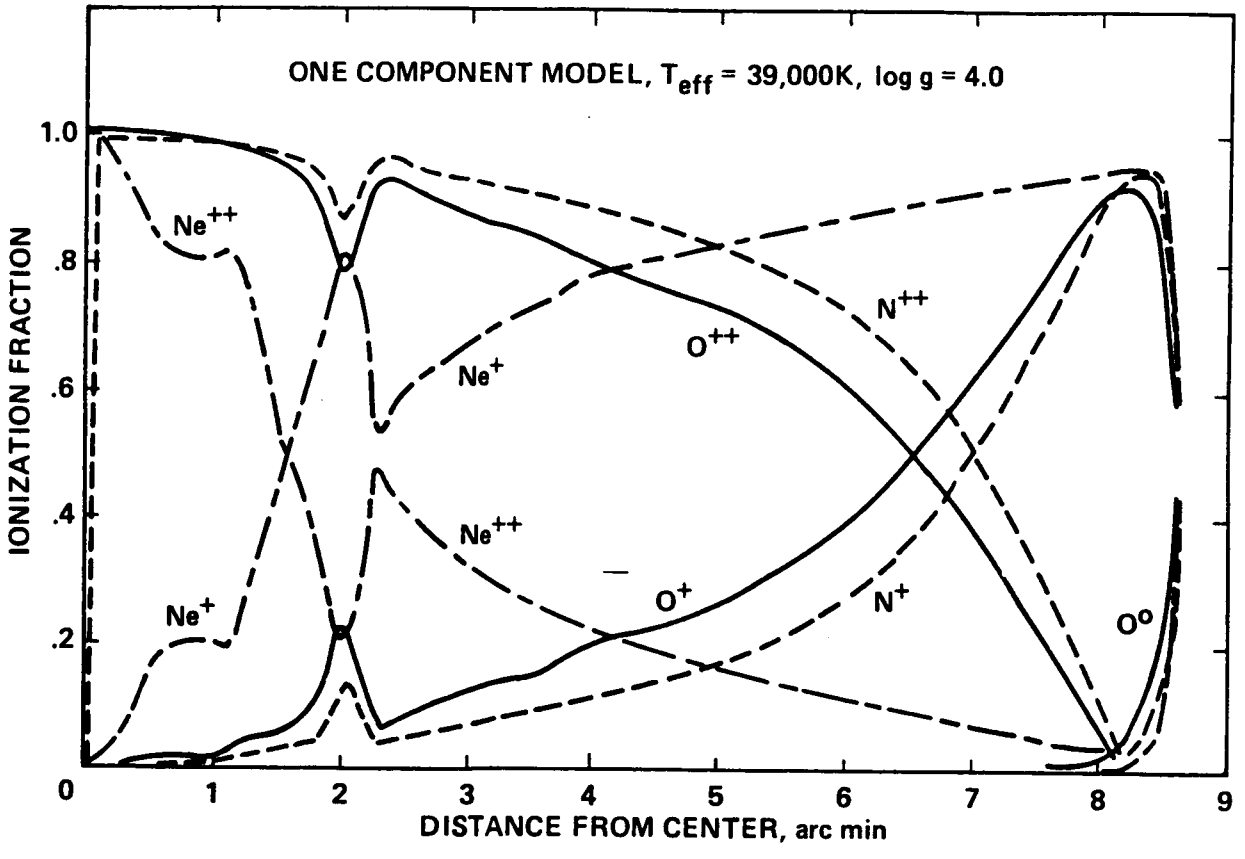

SIMPSON

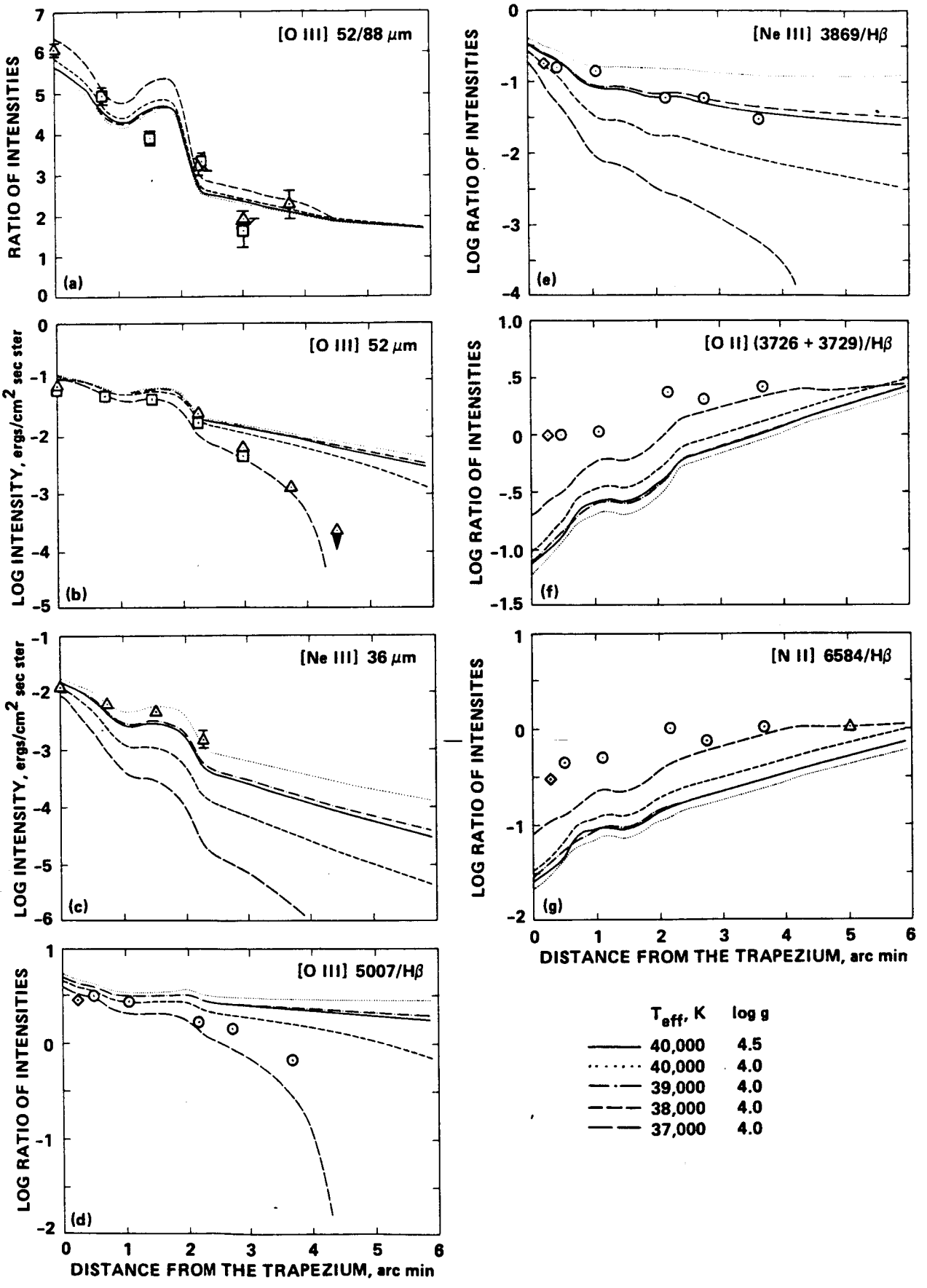
[O III] 52/88 μm
RATIO OF INTENSITIES
(a)
[O III] 52 μm
LOG INTENSITY, ergs/cm² sec ster
(b)
[Ne III] 36 μm
LOG INTENSITY, ergs/cm² sec ster
(c)
[O III] 5007/Hβ
LOG RATIO OF INTENSITIES
(d)
DISTANCE FROM THE TRAPEZIUM, arc min
[Ne III] 3869/Hβ
LOG RATIO OF INTENSITIES
(e)
[O II] (3726 + 3729)/Hβ
LOG RATIO OF INTENSITIES
(f)
[N II] 6584/Hβ
LOG RATIO OF INTENSITES
(g)
DISTANCE FROM THE TRAPEZIUM, arc min
T_eff, K
log g
40,000 4.5
40,000 4.0
39,000 4.0
38,000 4.0
37,000 4.0

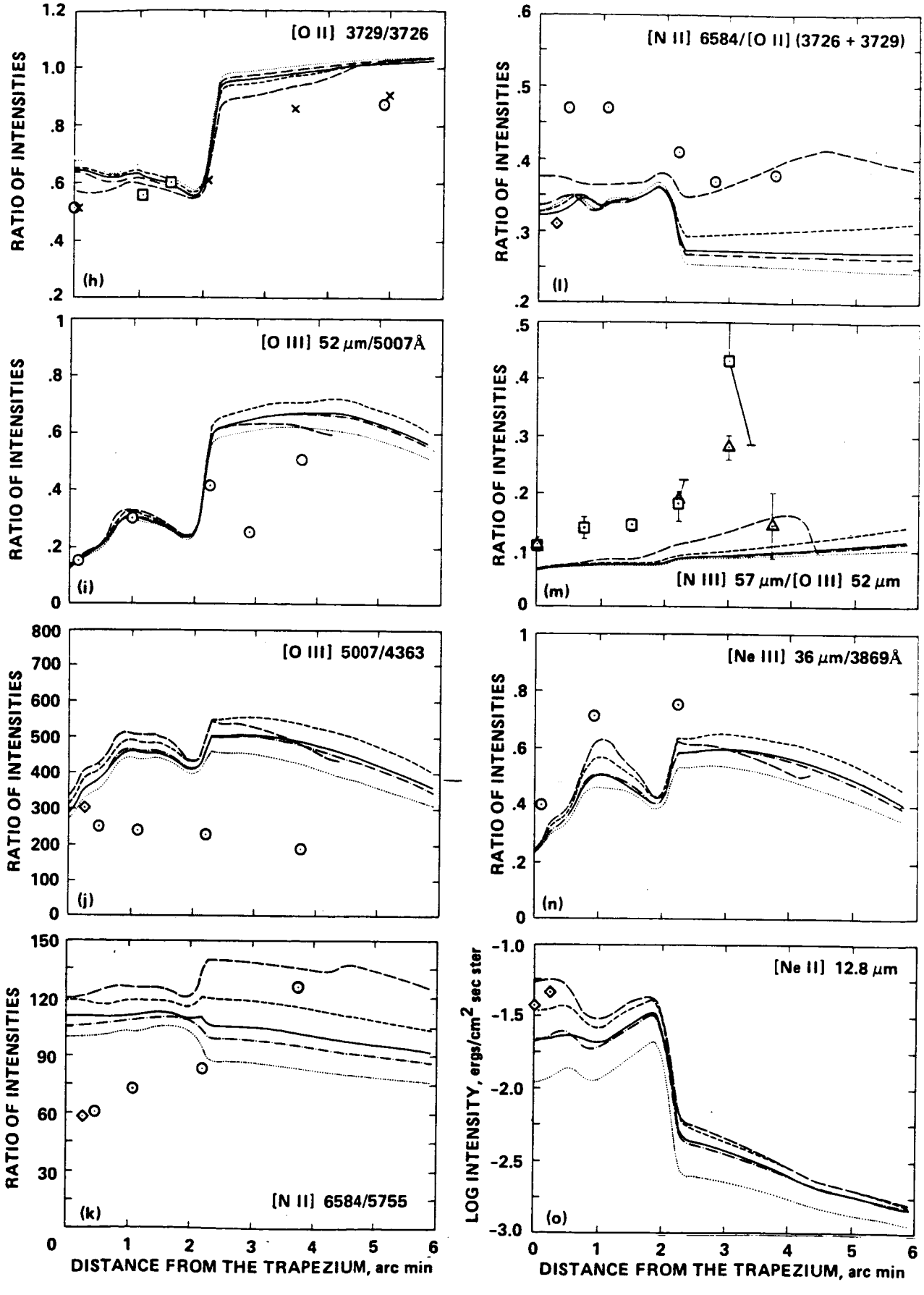
[O II] 3729/3726
(h)
[N II] 6584/[O II] (3726 + 3729)
(l)
[O III] 52 μm/5007Å
(i)
[N III] 57 μm/[O III] 52 μm
(m)
[O III] 5007/4363
(j)
[Ne III] 36 μm/3869Å
(n)
[N II] 6584/5755
(k)
[Ne II] 12.8 μm
(o)
RATIO OF INTENSITIES
LOG INTENSITY, ergs/cm^2 sec ster
DISTANCE FROM THE TRAPEZIUM, arc min

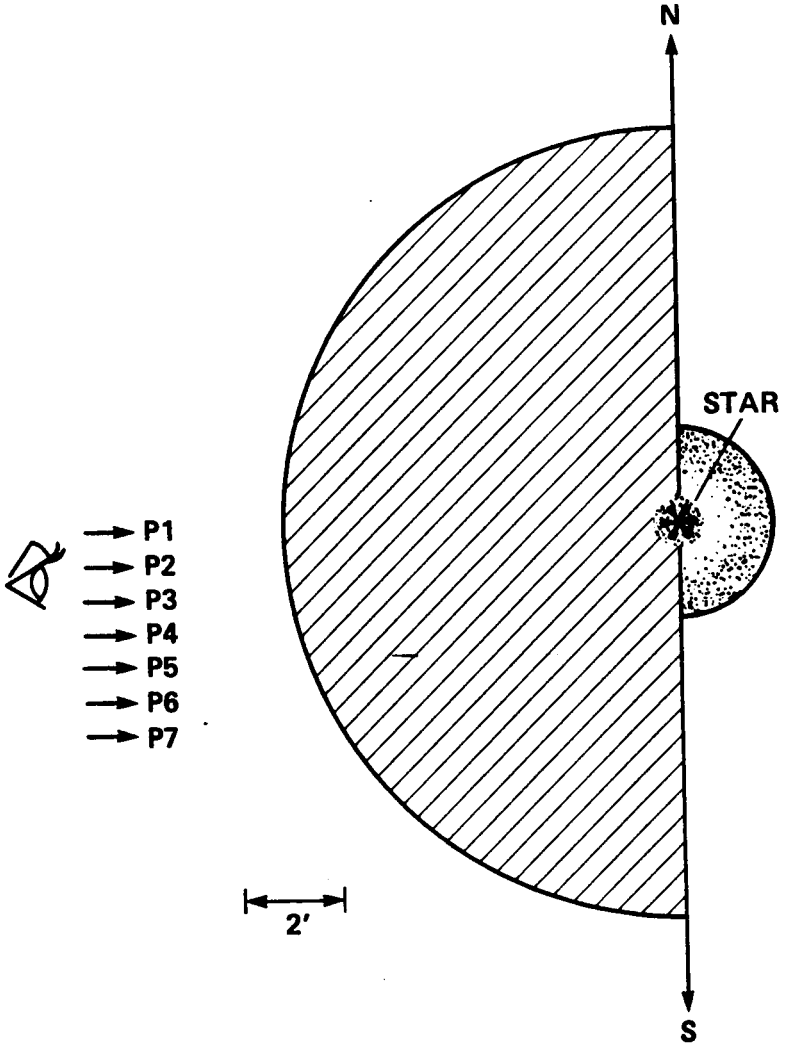

SIMPSON

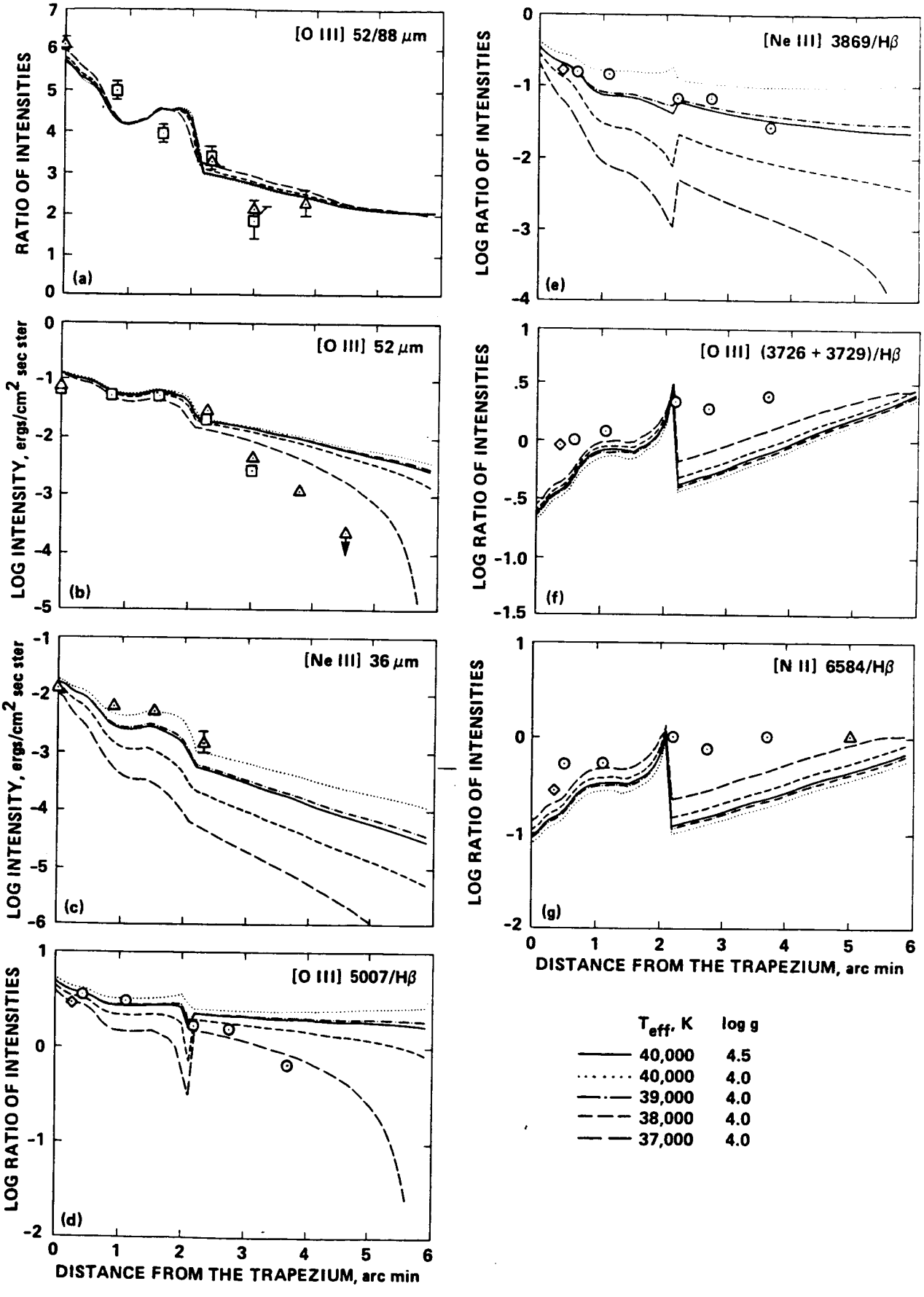
[O III] 52/88 μm
RATIO OF INTENSITIES
(a)
[O III] 52 μm
LOG INTENSITY, ergs/cm^2 sec ster
(b)
[Ne III] 36 μm
LOG INTENSITY, ergs/cm^2 sec ster
(c)
[O III] 5007/Hβ
LOG RATIO OF INTENSITIES
(d)
DISTANCE FROM THE TRAPEZIUM, arc min
[Ne III] 3869/Hβ
LOG RATIO OF INTENSITIES
(e)
[O III] (3726 + 3729)/Hβ
LOG RATIO OF INTENSITIES
(f)
[N II] 6584/Hβ
LOG RATIO OF INTENSITIES
(g)
DISTANCE FROM THE TRAPEZIUM, arc min
T_{eff}, K
log g
40,000 4.5
40,000 4.0
39,000 4.0
38,000 4.0
37,000 4.0

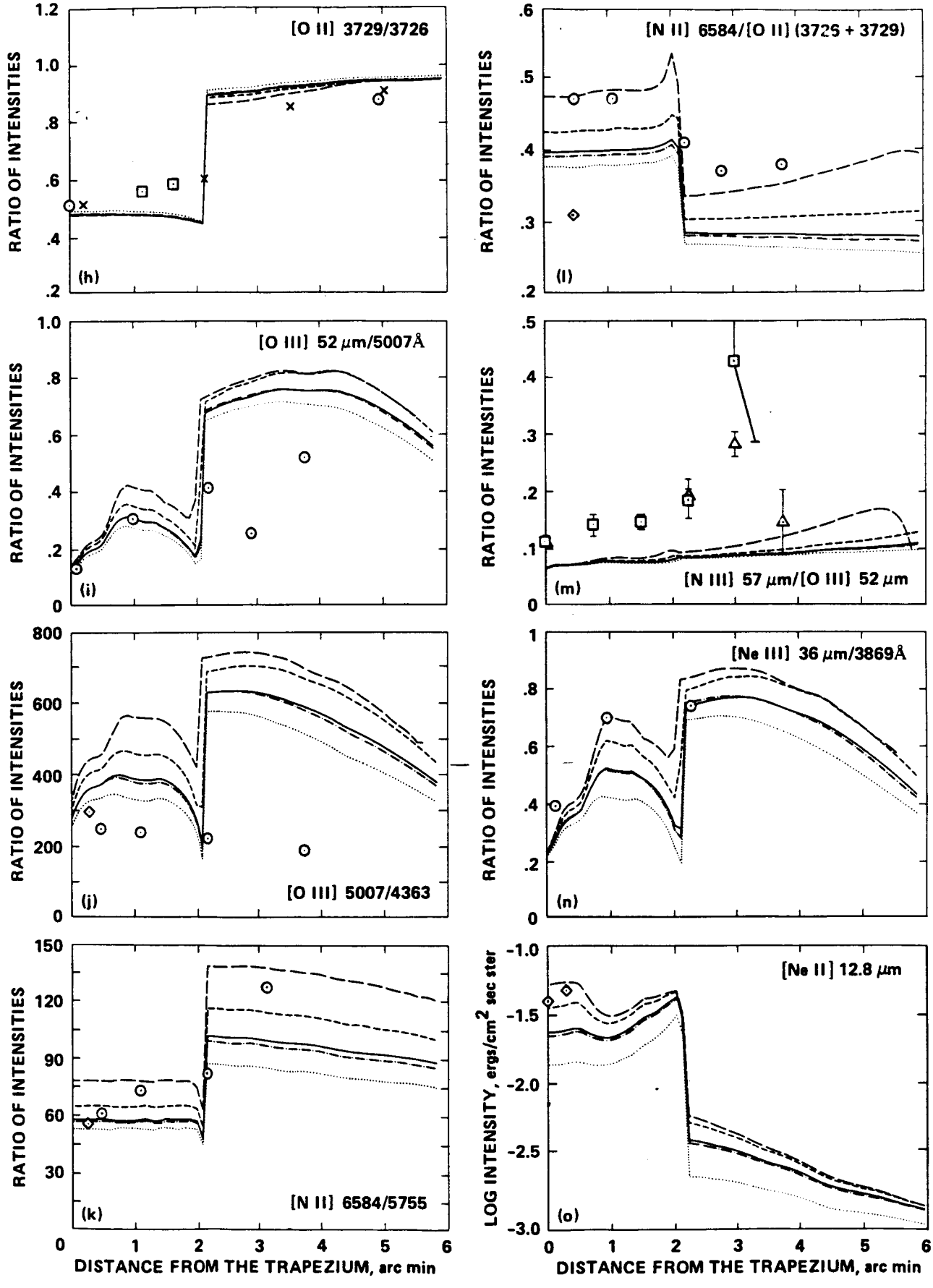
[O II] 3729/3726
(h)
[N II] 6584/[O II] (3729 + 3729)
(l)
[O III] 52 μm/5007Å
(i)
[N III] 57 μm/[O III] 52 μm
(m)
[O III] 5007/4363
(j)
[Ne III] 36 μm/3869Å
(n)
[N II] 6584/5755
(k)
[Ne II] 12.8 μm
(o)
RATIO OF INTENSITIES
LOG INTENSITY, ergs/cm^2 sec ster
DISTANCE FROM THE TRAPEZIUM, arc min

1. Report No.	2. Government Accession No.	3. Recipient's Catalog No.
NASA TM-88368		

4. Title and Subtitle	5. Report Date
THE IONIZATION STRUCTURE OF THE ORION NEBULA: INFRARED LINE OBSERVATIONS AND MODELS	October 1986
	6. Performing Organization Code

7. Author(s)	8. Performing Organization Report No.
J. P. Simpson,* R. H. Rubin,† E. F. Erickson,‡ and M. R. Haas§	A-86421
	10. Work Unit No.
9. Performing Organization Name and Address	
*Lick Observatory, University of California, Santa Cruz, CA 95064 †University of California, Los Angeles, CA 90024 ‡Ames Research Center, Moffett Field, CA 94035 §Mycol, Inc., Sunnyvale, CA 94087	11. Contract or Grant No.
	13. Type of Report and Period Covered
12. Sponsoring Agency Name and Address	Technical Memorandum
National Aeronautics and Space Administration Washington, DC 20546	14. Sponsoring Agency Code
	352-02-03

15. Supplementary Notes

Preprint Series #63. Supported by NASA grants.

Point of Contact: L. C. Haughney, Ames Research Center, MS 211-12, Moffett Field, CA 94035
(415)694-5339 or FTS 464-5339

16. Abstract

Observations of the [O III] 52 and 88 μm lines and the [N III] 57 μm line have been made at 6 positions and the [Ne III] 36 μm line at 4 positions in the Orion Nebula to probe its ionization structure. The measurements, made with a ~40" diameter beam, were spaced every 45" in a line south from and including the Trapezium. The wavelength of the [Ne III] line was measured to be 36.013 ±0.004 μm. Electron densities and abundance ratios of N^{++}/O^{++} have been calculated and compared to other radio and optical observations. Detailed one component and two component (bar plus halo) spherical models were calculated for exciting stars with effective temperatures of 37-40,000K and log g = 4.0 and 4.5. Both the new infrared observations and the visible line measurements of oxygen and nitrogen require $T_{eff} \lesssim 37{,}000$K. However, the doubly ionized neon requires a model with $T_{eff} \geq 39{,}000$K, which is more consistent with that inferred from the radio flux or spectral type. These differences in T_{eff} are not due to effects of dust on the stellar radiation field, but are probably due to inaccuracies in the assumed stellar spectrum. The observed N^{++}/O^{++} ratio is almost twice the N^{+}/O^{+} ratio. Our best fit models give $N/H = 8.4\times10^{-5}$, $O/H = 4.0\times10^{-4}$, and $Ne/H = 1.3\times10^{-4}$. Thus neon and nitrogen are approximately solar, but oxygen is half solar in abundance. From the infrared O^{++} lines we conclude that the ionization bar results from an increase in column depth rather than from a local density enhancement.

17. Key Words (Suggested by Author(s))	18. Distribution Statement
Nebulae: H II regions Nebulae: Orion nebulae Nebulae: abundances	Unclassified - Unlimited Subject Category - 89

19. Security Classif. (of this report)	20. Security Classif. (of this page)	21. No. of Pages	22. Price*
Unclassified	Unclassified	37	A02

*For sale by the National Technical Information Service, Springfield, Virginia 22161